Available at
www.ComputerScienceWeb.com
POWERED BY SCIENCE DIRECT®

ELSEVIER

Neurocomputing 52–54 (2003) 933–942

NEUROCOMPUTING

www.elsevier.com/locate/neucom

Computational modeling of bursting pacemaker neurons in the pre-Bötzinger complex

N.A. Shevtsova[a,*], K. Ptak[b], D.R. McCrimmon[b], I.A. Rybak[a]

[a] *School of Biomedical Engineering, Science and Health Systems, Drexel University, 3141 Chestnut Street, Philadelphia, PA 19104, USA*

[b] *Department of Physiology and Institute for Neuroscience, Feinberg School of Medicine, Northwestern University, Chicago, IL 60611-3008, USA*

Abstract

Bursting pacemaker neurons in the pre-Bötzinger complex (pBC) were modeled in the Hodgkin–Huxley style. The single neuron model included rapidly inactivating sodium, persistent sodium, and delayed-rectifier potassium currents. The kinetics of the rapidly inactivating and persistent sodium channels was modeled using experimental data obtained from whole-cell patch clamp recordings from pBC neurons in vitro. Our computational study focused on the conditions that could provide the generation of endogenous bursting activity in single pacemaker neurons and neural populations and on the specific roles of voltage-gated potassium and persistent sodium currents in triggering or suppression of endogenous population oscillations in the pBC.

Keywords: Computational modeling; Pre-Bötzinger complex; Endogenous oscillations; Potassium channels; Respiratory rhythm

1. Introduction

The pre-Bötzinger complex (pBC) is a region in the rostroventrolateral medulla that is considered an important part of the respiratory neural network [1–4,11,12,20,25,27]. As shown in vitro, this region, under certain conditions, can generate an intrinsic rhythmic bursting activity [3,11,12,20,25,27] that is resistant to blockade of synaptic inhibition [23]. It has been suggested, that this in vitro activity is driven by a

* Corresponding author.
E-mail address: natalia@cbis.ece.drexel.edu (N.A. Shevtsova).

0925-2312/03/$ - see front matter
doi:10.1016/S0925-2312(02)00841-X

sub-population of pacemaker neurons located in the pBC [1–3,11,20]. The theoretical analysis of possible intrinsic cellular mechanisms led to the suggestion that this endogenous rhythm is generated with a necessary contribution of the persistent sodium current [1,2] (for an opposite view see [4]). This current was recently described in pBC neurons [10,16,19,24] and its voltage-dependent properties were characterized [19,24].

Our computational study focused on the investigation of the possible conditions that may define the generation of pacemaker-driven oscillations in the pBC and on studying the possible roles of persistent sodium and voltage-gated potassium currents in triggering these endogenous oscillations.

2. Model description

A model of a single pBC pacemaker neuron was developed using the Hodgkin–Huxley formalism. The model was based on previous models [1–3]. However, in contrast to these models based on generic descriptions of sodium channels, we incorporated voltage-gated and kinetic parameters for sodium currents drawn from our in vitro studies of isolated pBC neurons [19,24].

The following ionic currents (and the corresponding channel conductances) were incorporated into the model: rapidly inactivating (fast) sodium (I_{Naf} with maximal conductance $\bar{g}_{\mathrm{Naf}}$); persistent sodium (I_{NaP} with maximal conductance $\bar{g}_{\mathrm{NaP}}$); delayed-rectifier potassium (I_{K} with maximal conductance $\bar{g}_{\mathrm{K}}$); leakage (I_{leak} with constant conductance g_{leak}), and synaptic excitatory (I_{synE} with conductance g_{synE}) and inhibitory (I_{synI} with conductance g_{synI}) currents, which together defined the dynamics of the neuron membrane potential. The voltage-gated and kinetic parameters for I_{Naf} and I_{NaP} were drawn from our in vitro studies [19,24]. The mean values of the maximal sodium conductances used in the model ($\bar{g}_{\mathrm{Naf}} = 150$ nS and $\bar{g}_{\mathrm{NaP}} = 4$ nS) were also set based our experimental measurements ($\bar{g}_{\mathrm{Naf}} = 34$–$170$ nS and $\bar{g}_{\mathrm{NaP}} = 0.5$–$5$ nS; see [19,24]). Similar to Model 1 by Butera et al. [1], the persistent sodium channel in our model had slow inactivation. Because the delayed-rectifier potassium channels have not been characterized in the pBC and other respiration related areas, we used the formal descriptions of this channel taken and adapted from the model of thalamocortical neurons by McCormick and Huguenard [15]. The mean value of $\bar{g}_{\mathrm{K}}$ was set to 50 nS. The reversal potentials for sodium and potassium currents were calculated using the Nernst equation, and the leakage reversal potential was obtained using the Goldman equation. The value of the whole-cell capacitance, $C = 36.2$ pF, was set from experimental data obtained on neurons dissociated from the rostral ventrolateral medulla of rat [9]. The mean value of the leakage conductance, $g_{\mathrm{leak}} = 2$ nS, was set to fit the experimentally measured input resistance $R_{\mathrm{in}} = 500$ MΩ [14].

To investigate firing behavior of pacemaker neuron populations we modeled a population of 50 neurons with all-to-all excitatory synaptic connections. Heterogeneity within the modeled neural population was set by random distribution of the maximal channel conductances ($\bar{g}_{\mathrm{NaP}}$, $\bar{g}_{\mathrm{K}}$ and g_{leak}), values of the external excitatory drive (g_{Edr}) and weights of the synaptic interconnections within the population (w_{ij}).

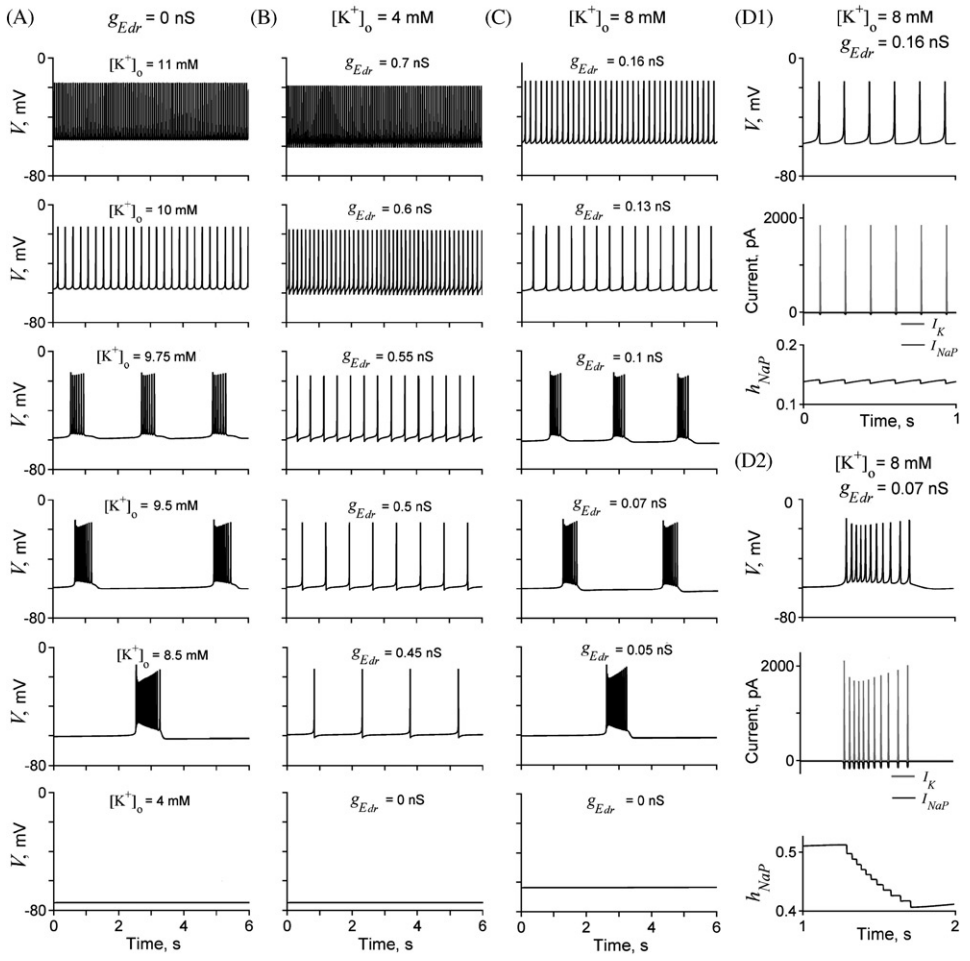

Fig. 1. Firing activity of a model of pBC pacemaker neuron under different conditions. (A) Firing behavior of the model without excitatory drive ($g_{\mathrm{Edr}} = 0$) at different levels of extracellular potassium concentration ($[K^+]_0$). $[K^+]_0$ increases bottom-up. An increase of $[K^+]_0$ triggers the rhythmic bursting activity at some threshold of $[K^+]_0$. Further increase in $[K^+]_0$ increases burst frequency and decreases burst duration. At a high level of $[K^+]_0$, bursting switches to tonic firing. (B) Firing behavior of the model at $[K^+]_0 = 4$ mM. g_{Edr} increases bottom-up. An increase in g_{Edr} causes an increase in the tonic firing frequency. Note the absence of bursting activity at any value of g_{Edr}. (C) Firing behavior of the model at $[K^+]_0 = 8$ mM. g_{Edr} increases bottom-up. Busting activity is triggered when g_{Edr} exceeds some threshold. The frequency of bursts increases with an increase of g_{Edr} until the neuron switches to tonic firing at a higher level of g_{Edr}. (D1) and (D2) Dynamics of the neuronal membrane potential (V, top trace), the persistent sodium (I_{NaP}, middle trace, black) and delayed-rectifier (I_{K}, middle trace, gray) currents, and the persistent sodium inactivation variable h_{NaP} (bottom trace) during tonic activity (D1) and bursting (D2).

3. Results

The model of a single pBC pacemaker neuron demonstrated the ability to generate endogenous bursting activity under certain conditions (within a particular area in the parameter space). Fig. 1A shows that an increase in extracellular potassium concentration ($[K^+]_0$) triggered a rhythmic bursting activity at some threshold of $[K^+]_0$. A further increase in $[K^+]_0$ increased burst frequency and decreased burst duration, and then, at a higher $[K^+]_0$, bursting switched to tonic firing (Fig. 1A). An increase in excitatory tonic drive to the neuron (g_{Edr}) at the basic level of $[K^+]_0$ (4 mM) did not produce bursting, but increased the tonic firing frequency (Fig. 1B). At a higher level of $[K^+]_0$ (e.g. at $[K^+]_0 = 8$ mM, Fig. 1C), busting activity was triggered when g_{Edr} exceeded some threshold. The frequency of bursts increased with an increase of g_{Edr} until the neuron switched to tonic firing at a high level of g_{Edr} (Fig. 1C). As described in detail by Butera et al. [1], the burst generation mechanism in this type of bursting pacemaker neuron model is explicitly dependent on the slow voltage-dependent inactivation of the persistent sodium current (h_{NaP}), which increases slowly during interburst periods and decreases during bust periods (Fig. 1D2). Comparison of the amplitudes of I_{NaP} and I_K during spikes showed that both the I_{NaP} amplitude and the ratio of amplitudes I_{NaP}/I_K is much higher in the bursting mode than in the mode of tonic activity (Figs. 1D1, 1D2).

To investigate firing behavior of a population of pacemaker neurons we modeled a population of 50 neurons with all-to-all excitatory synaptic connections. Our simulation showed that both an increase in the weights of excitatory synaptic interconnections and a randomization of neuronal parameters within the population increased the area of the parameter space that produced population busting compared to that for a single pacemaker neuron (see also [2,3]). Fig. 2 shows an example of our simulations at the population level. An increase of $[K^+]_0$ above some threshold (about 7.5 mM) triggered synchronized bursting activity in the population. Further elevation of $[K^+]_0$ produced increased burst frequency and decreased burst amplitude. At a higher level of $[K^+]_0$, the population bursting activity switched to high-frequency asynchronous firing (Fig. 2A). An increase of the g_{Edr} at the basic level of $[K^+]_0$ (4 mM) did not produce population bursting, but only increased the level of asynchronous activity (Fig. 2B). At higher values of $[K^+]_0$ (e.g. at $[K^+]_0 = 6$ mM, see Fig. 2C), population busting was triggered when g_{Edr} exceeded some threshold. The frequency of bursts increased with

Fig. 2. Firing activity of a model of population of pacemaker neurons under different conditions. The result of each simulation is represented by two diagrams: the top diagram is a raster plot for spike times in all 50 cells, sorted on the ordinate axis by cell index number; the bottom diagram is a corresponding integrated histogram of population activity (bin size = 10 ms). (A) An example of firing behavior of the model without excitatory drive ($g_{Edr} = 0$) at different $[K^+]_0$. $[K^+]_0$ increases bottom-up. An increase of $[K^+]_0$ triggers rhythmic bursting activity in the population at some threshold of $[K^+]_0$. A further increase in $[K^+]_0$ increases burst frequency and decreases burst amplitude. At a higher level of $[K^+]_0$, firing activity switches to asynchronous firing. (B) An example of firing behavior of the model at $[K^+]_0 = 4$ mM. Mean value of g_{Edr} in the population increases bottom-up. Note the absence of bursting at any value of g_{Edr}. (C) An example of firing behavior of the model at $[K^+]_0 = 6$ mM. Busting activity is triggered when g_{Edr} exceeds some threshold. At a higher level of g_{Edr} population activity switches to asynchronous firing.

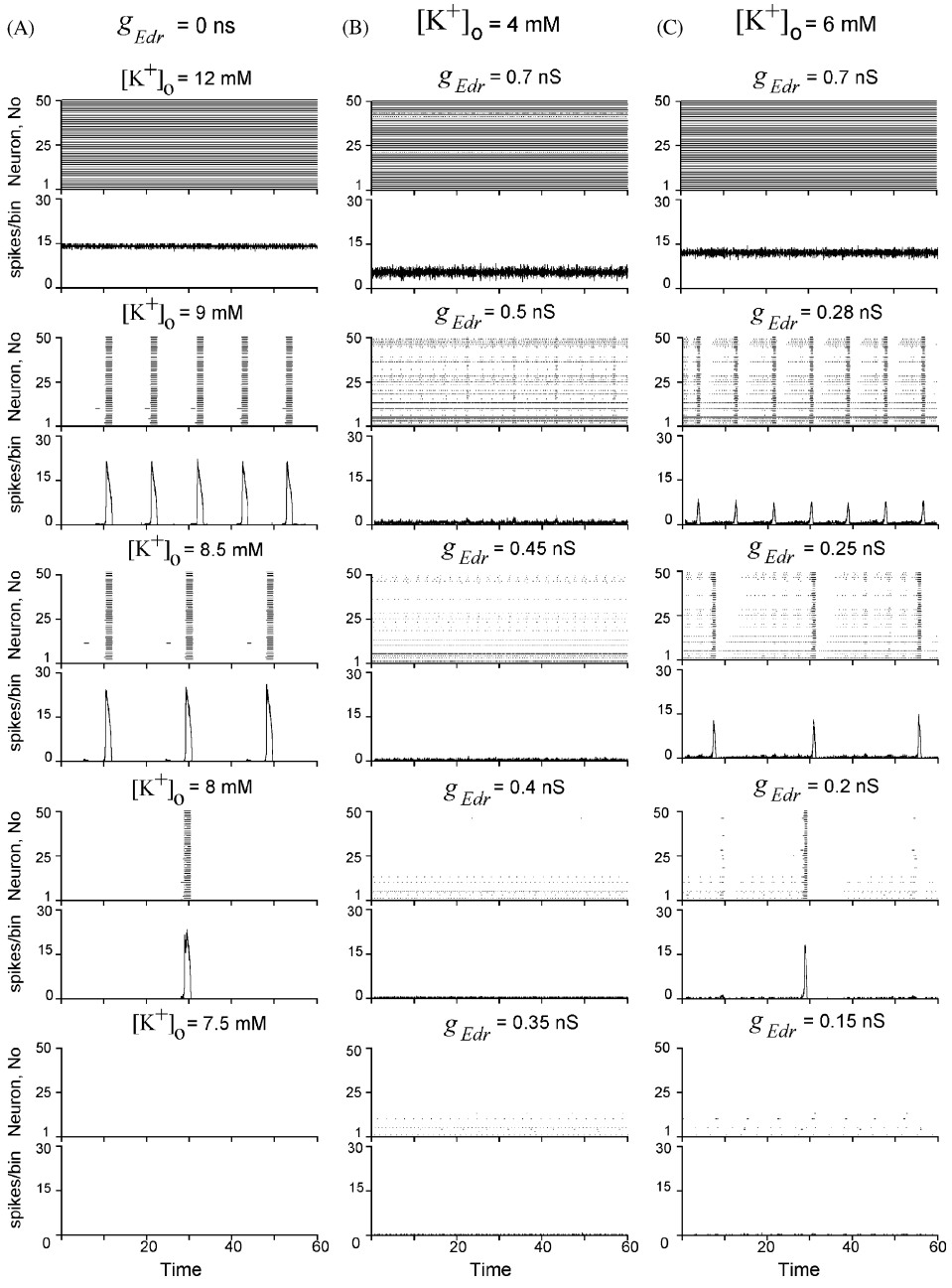
(A)
g_{Edr} = 0 ns
$[K^+]_o$ = 12 mM
$[K^+]_o$ = 9 mM
$[K^+]_o$ = 8.5 mM
$[K^+]_o$ = 8 mM
$[K^+]_o$ = 7.5 mM
(B)
$[K^+]_o$ = 4 mM
g_{Edr} = 0.7 nS
g_{Edr} = 0.5 nS
g_{Edr} = 0.45 nS
g_{Edr} = 0.4 nS
g_{Edr} = 0.35 nS
(C)
$[K^+]_o$ = 6 mM
g_{Edr} = 0.7 nS
g_{Edr} = 0.28 nS
g_{Edr} = 0.25 nS
g_{Edr} = 0.2 nS
g_{Edr} = 0.15 nS
Neuron, No
spikes/bin
Time

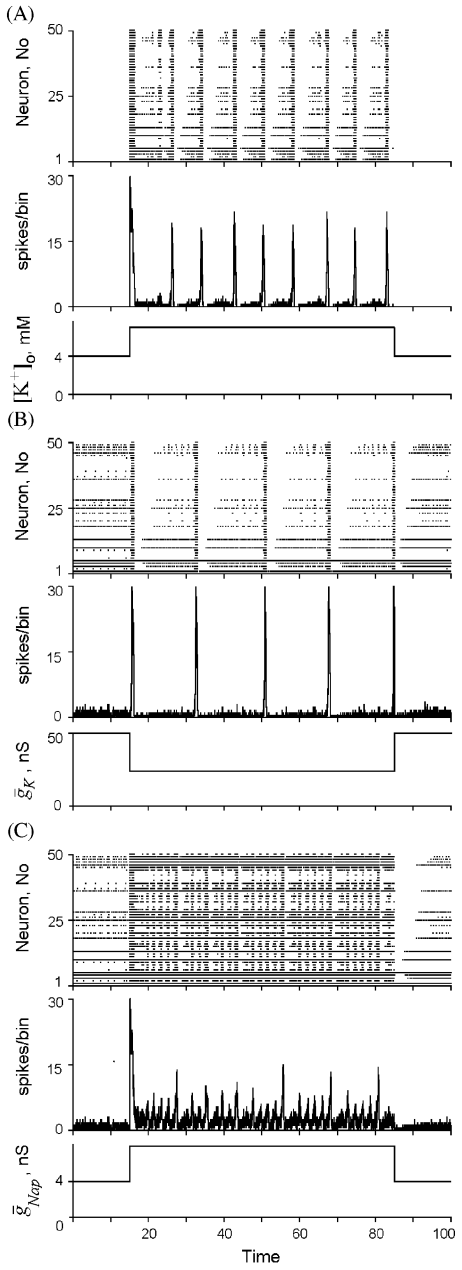

Fig. 3. Triggering endogenous bursting activity in the model of a population of pacemaker neurons. (A) An example of triggering endogenous bursting activity by elevation of $[K^+]_0$ (bottom traces). $[K^+]_0$ was increased from 4 to 8 mM. (B) An example of triggering endogenous bursting activity by reduction of the mean value of $\bar{g}_K$ in the population. The mean value of $\bar{g}_K$ was reduced from 50 to 25 nS to. (C) An example of triggering endogenous bursting activity by augmentation of the mean value of $\bar{g}_{NaP}$. The mean value of $\bar{g}_{NaP}$ was increased from 4 to 7 nS.

an increase in g_{Edr}. Finally, at some level of g_{Edr}, firing behavior of the population switched to high-frequency asynchronous firing (Fig. 2C).

The important conclusion from our modeling studies is that an increase of excitatory drive to the neuron and an increase of $[K^+]_0$ produce different effects on neuronal and population firing behavior. Specifically, an increase of excitatory drive at a normal physiological level of $[K^+]_0$ causes cellular depolarization without changing a balance between I_{NaP} and I_K. In this case, the normally expressed I_K provides sufficient membrane repolarization after each generated spike to reduce the membrane potential below the level of I_{NaP} activation and does not permit endogenous oscillations. In contrast, an increase of $[K^+]_0$ produces two simultaneous effects: one is the cellular depolarization (via shifting the leakage reversal potential to more positive values of voltage); the other is the reduction of I_K by shifting the potassium reversal potential to more positive values of voltage. Therefore, at higher levels of $[K^+]_0$, the reduced I_K does not produce a sufficient postspike repolarization and hence cannot restrain endogenous I_{NaP}-dependent bursting activity.

In this study, we focused on the investigation of the specific roles of the I_K and I_{NaP} in inducing or suppressing endogenous population bursting activity. Fig. 3 shows examples of our simulations. Elevation of $[K^+]_0$ from the basic level of 4–8 mM triggered bursting activity in the population. This bursting activity stopped when $[K^+]_0$ returned to the basic level (Fig. 3A). At the same time, the synchronized population bursting could also be triggered at $[K^+]_0 = 4$ mM by a reduction of $\bar{g}_K$ (Fig. 3B) or an augmentation of $\bar{g}_{NaP}$ (Fig. 3C).

4. Conclusion and discussion

In summary, our modeling studies demonstrate that rhythmic bursting activity in a population of pacemaker neurons may be initiated by (1) an increase of the extracellular potassium concentration, or (2) a suppression of the voltage-gated potassium currents, or (3) an augmentation of the persistent sodium currents.

This conclusion is consistent with the majority of in vitro studies of endogenous rhythmic activity in the pBC, in which the researchers elevated $[K^+]_0$ to 7–9 mM in order to trigger and maintain a robust activity, e.g. see [11,12,27]. Our modeling predictions was recently confirmed by Pierrefiche et al. [18], who demonstrated that rhythmic bursting in the medullary slice could be triggered either by elevation of $[K^+]_0$ to 7 mM, or by application of different potassium current blockers (TEA or 4-AP) at $[K^+]_0 = 3$ mM.

Our results are also consistent with the suggestion that gasping during hypoxia is produced by a pacemaker-driven mechanism in the pBC [21,22,26]. Specifically, hypoxia is accompanied by elevation of $[K^+]_0$ [17], suppression of voltage-gated potassium currents [5,8,13], and augmentation of I_{NaP} [6,7,9], which are the same factors that produced the population oscillations in our modeling studies. The results of a recent study of the neurogenesis of gasping in situ [26] are also consistent with this idea. Specifically, application of 4-AP and strychnine in combination with an increase of $[K^+]_0$ converted the eupneic pattern of phrenic nerve discharge to a decrementing discharge similar to that recorded both in vitro and during ischemia-induced gasping in situ [26].

Acknowledgements

This work was supported by NSF (0091942) and ONR (N000140010719) grants to I.A. Rybak and NIH grants HL60097 and HL60969 to D.R. McCrimmon.

References

[1] R.J. Butera, J.R. Rinzel, J.C. Smith, Models of respiratory rhythm generation in the pre-Bötzinger complex: I. Bursting pacemaker neurons, J. Neurophysiol. 82 (1999) 382–397.
[2] R.J. Butera, J.R. Rinzel, J.C. Smith, Models of respiratory rhythm generation in the pre-Bötzinger complex: II. Populations of coupled pacemaker neurons, J. Neurophysiol. 82 (1999) 398–415.
[3] C.A. Del Negro, S.M. Johnson, R.J. Butera, J.C. Smith, Models of respiratory rhythm generation in the pre-Bötzinger complex: III. Experimental tests of model predictions, J. Neurophysiol. 86 (2001) 59–74.
[4] C.A. Del Negro, C. Morgado-Valle, J.L. Feldman, Respiratory rhythm: an emergent network property? Neuron 34 (2002) 821–830.
[5] C. Gebhardt, U. Heinemann, Anoxic decrease in potassium outward currents of hippocampal cultured neurons in absence and presence of dithionite, Brain Res. 837 (1999) 270–276.
[6] A.K. Hammarström, P.W. Gage, Inhibition of oxidative metabolism increases persistent sodium current in rat CA1 hippocampal neurons, J. Physiol. London 510 (1998) 735–741.
[7] E.M. Horn, T.G. Waldrop, Hypoxic augmentation of fast-inactivating and persistent sodium currents in rat caudal hypothalamic neurons, J. Neurophysiol. 84 (2000) 2572–2581.
[8] C. Jiang, G.G. Haddad, A direct mechanism for sensing low oxygen levels by central neurons, Proc. Natl. Acad. Sci. USA 91 (1994) 7198–7201.
[9] Y. Kawai, J. Qi, A.H. Comer, H. Gibbons, J. Win, J. Lipski, Effects of cyanide and hypoxia on membrane currents in neurons acutely dissociated from the rostral ventrolateral medulla of the rat, Brain Res. 830 (1999) 246–257.
[10] N. Koshiya, C. Del Negro, R.J. Butera, J.C. Smith, Persistent sodium current (INaP) in pre-pre-Bötzinger complex (pre-BötC) inspiratory neurons, Soc. Neurosci. Abs. 27 (2001) 243.3.
[11] N. Koshiya, J.C. Smith, Neuronal pacemaker for breathing visualized in vitro, Nature 400 (1999) 360–363.
[12] S.P. Lieske, M. Thoby-Brisson, P. Telgkamp, J.M. Ramirez, Reconfiguration of the neural network controlling multiple breathing patterns: eupnea, sighs and gasps, Nature Neurosci. 3 (2000) 600–607.
[13] J. Lopez-Barneo, R. Pardal, P. Ortega-Saenz, Cellular mechanisms of oxygen sensing, Annu. Rev. Physiol. 63 (2001) 259–287.
[14] E. Mazza Jr., N.H. Edelman, J.A. Neubauer, Hypoxic excitation in neurons cultured from the rostral ventrolateral medulla of the neonatal rat, J. Appl. Physiol. 88 (2000) 2319–2329.
[15] D.A. McCormick, J.R. Huguenard, A model of the electrophysiological properties of thalamocortical relay neurons, J. Neurophysiol. 68 (1992) 1384–1400.
[16] D.R. McCrimmon, A. Monnier, K. Ptak, G. Zummo, Z. Zhang, G.F. Alheid, Respiratory rhythm generation: pre-Bötzinger neuron discharge patterns and persistent sodium current, Adv. Exp. Med. Biol. 499 (2001) 147–152.
[17] J.E. Melton, S.C. Kadia, Q.P. Yu, J.A. Neubauer, N.H. Edelman, Respiratory and sympathetic activity during recovery from hypoxic depression and gasping in cats, J. Appl. Physiol. 80 (1996) 1940–1948.
[18] O. Pierrefiche, I.A. Rybak, W.M. St.-John, J.F.R. Paton, Neurogenesis of respiratory rhythm: effects of suppression of potassium currents and hypoxia, Soc. Neurosci. Abs. 28 (2002) 173.11.
[19] K. Ptak, G. Zummo, G.F. Alheid, J.D. Surmeier, D.R. McCrimmon, Biophysical and molecular properties of persistent sodium current in pre-Bötzinger complex respiratory neurons, Soc. Neurosci. Abs. 28 (2002) 221.8.
[20] J.C. Rekling, J.L. Feldman, Pre-Bötzinger complex and pacemaker neurons: hypothesized site and kernel for respiratory rhythm generation, Annu. Rev. Physiol. 60 (1998) 385–405.
[21] I.A. Rybak, J.F.R. Paton, R.F. Rogers, W.M. St.-John, Generation of the respiratory rhythm: state-dependency and switching, Neurocomputing 44–46 (2002) 605–614.

[22] I.A. Rybak, W.M. St.-John, J.F.R. Paton, Models of neuronal bursting behavior: implications for in vivo versus in vitro respiratory rhythmogenesis, Adv. Exp. Med. Biol. 499 (2001) 159–164.
[23] X.M. Shao, J.L. Feldman, Respiratory rhythm generation and synaptic inhibition of expiratory neurons in pre-Bötzinger complex: differential roles of glycinergic and gabaergic neural transmission, J. Neurophysiol. 77 (1997) 1853–1860.
[24] N.A. Shevtsova, K. Ptak, D.R. McCrimmon, I.A. Rybak, Study on sodium current in neurons of pre-Bötzinger complex (pBC), Soc. Neurosci. Abs. 28 (2002) 173.5.
[25] J.C. Smith, H.H. Ellenberger, K. Ballanyi, D.W. Richter, J.L. Feldman, Pre-Bötzinger complex: a brainstem region that may generate respiratory rhythm in mammals, Science 254 (1991) 726–729.
[26] W.M. St.-John, I.A. Rybak, J.F.R. Paton, Potential switch from eupnea to fictive gasping following blockade of glycine transmission and potassium channels, Am. J. Physiol. (Integr. Comp. Physiol.) 283 (2002) R721–R731.
[27] M. Thoby-Brisson, J.M. Ramirez, Identification of two types of inspiratory pacemaker neurons in the isolated respiratory network of mice, J. Neurophysiol. 86 (2001) 104–112.

Natalia A. Shevtsova started her scientific carrier in 1974 in AB Kogan Research Institute for Neurocybernetics at Rostov State University (Russia). She was a senior researcher in Ilya Rybak's group in 1972–1991. In 1992 she received "The Best Paper Award" from "Neurocomputing" for her work on neural network model of visual perception. She received a Ph.D. in Computer Science from Rostov State University in 1996. In 1996–1998 she was a research associate in James Reggia's group at the University of Maryland (College Park, MD). From 2001 she is a research associate in Ilya Rybak's group at the School of Biomedical Engineering, Science and Health Systems, Drexel University, Philadelphia, PA. Her research interests include computational modeling of biological neurons and neural networks, neural control of respiration and visual perception.

Krzysztof Ptak graduated in 1996 from Jagiellonian University in Cracow. After graduating, he joined Roger Monteau's group at the Aix-Marseille University. In 1999 he received a Ph.D. for "Substance P and modulation of central respiratory activity: in vitro study on rodents in the perinatal period" from both Aix-Marseille and Jagiellonian Universities. This work was awarded by the Prime Minister of the Polish government as the best doctoral thesis in 1999. He is currently a research associate in Donald McCrimmon's group at the Feinberg School of Medicine at Northwestern University in Chicago, IL. Presently he is studying the role of sodium conductance in generation of pacemaker activity in medullary pre-Bötzinger Complex neurons using patch-clamp recording and single-cell RT-PCR techniques.

Donald R. McCrimmon studied exercise physiology at the University of Calgary, Canada. After graduating in 1974, he joined David Cunningham's group at the University of Western Ontario and received an M.A. in 1976 for comparing the effects of intermittent versus continuous exercise training regimens on the cardiopulmonary systems. He then began work on the central neural control of breathing at the University of Wisconsin in Madison under the tutelage of Jerome Dempsey and Peter Lalley. After receiving a Ph.D. in Physiology in 1983 he traveled to Northwestern University in Chicago where he began postdoctoral work with Jack Feldman and in 1986 established a laboratory to study brainstem pathways controlling respiratory rhythm and pattern. He is currently an Associate Professor and Associate Chair of the Department of Physiology at Feinberg School of Medicine, Northwestern University (Chicago, IL).

Ilya A. Rybak received a Ph.D. in Biophysics from St. Petersburg University in 1988. In 1977–1991 he was a senior researcher and head of the lab for Neural Network Modeling in Vision Research in AB Kogan Research Institute for Neurocybernetics at Rostov State University (Russia). In 1992 he received "The Best Paper Award" from "Neurocomputing" for his work on neural network model of visual perception. In 1993–1998 he was a visiting scientist at the Central Research Department at the DuPont Company. He is currently a Research Professor at the School of Biomedical Engineering, Science and Health Systems, Drexel University, Philadelphia, PA. His scientific interests include computational modeling of biological neurons and neural networks with a research focus on neural control of respiration and locomotion, visual perception, biologically inspired robotics and brain–machine interfaces.